Biochemical and Biophysical Research Communications 391 (2010) 703–708

Contents lists available at ScienceDirect

Biochemical and Biophysical Research Communications

journal homepage: www.elsevier.com/locate/ybbrc

1.45 Å resolution crystal structure of recombinant PNP in complex with a pM multisubstrate analogue inhibitor bearing one feature of the postulated transition state

Grzegorz Chojnowski [a,b], Katarzyna Breer [a], Marta Narczyk [a], Beata Wielgus-Kutrowska [a], Honorata Czapinska [b], Mariko Hashimoto [c], Sadao Hikishima [c], Tsutomu Yokomatsu [c], Matthias Bochtler [b,d,e], Agnieszka Girstun [f], Krzysztof Staroń [f], Agnieszka Bzowska [a,*]

[a] Department of Biophysics, Institute of Experimental Physics, University of Warsaw, Żwirki i Wigury 93, 02-089 Warsaw, Poland
[b] International Institute of Molecular and Cell Biology, Trojdena 4, 02-109 Warsaw, Poland
[c] School of Pharmacy, Tokyo University of Pharmacy and Life Sciences, 1432-1 Horinouchi, Hachioji, Tokyo 192-0392, Japan
[d] Schools of Chemistry and Biosciences, Park Place, CF10 3AT Cardiff, United Kingdom
[e] Max Planck Institute of Molecular Cell Biology and Genetics, Pfotenhauerstr. 108, 01309 Dresden, Germany
[f] Department of Molecular Biology, Institute of Biochemistry, University of Warsaw, Miecznikowa 1, 02-096 Warsaw, Poland

ARTICLE INFO

Article history:
Received 12 November 2009
Available online 26 November 2009

Keywords:
Calf purine nucleoside phosphorylase
Third-of-the-sites binding
X-ray crystallography
Multisubstrate inhibitor
Transition state
Fluorimetric titrations

ABSTRACT

Low molecular mass purine nucleoside phosphorylases (PNPs, E.C. 2.4.2.1) are homotrimeric enzymes that are tightly inhibited by immucillins. Due to the positive charge on the ribose like part (iminoribitol moiety) and protonation of the N7 atom of the purine ring, immucillins are believed to act as transition state analogues. Over a wide range of concentrations, immucillins bind with strong negative cooperativity to PNPs, so that only every third binding site of the enzyme is occupied (third-of-the-sites binding). 9-(5′,5′-difluoro-5′-phosphonopentyl)-9-deazaguanine (DFPP-DG) shares with immucillins the protonation of the N7, but not the positive charge on the ribose like part of the molecule. We have previously shown that DFPP-DG interacts with PNPs with subnanomolar inhibition constant. Here, we report additional biochemical experiments to demonstrate that the inhibitor can be bound with the same K_d (~190 pM) to all three substrate binding sites of the trimeric PNP, and a crystal structure of PNP in complex with DFPP-DG at 1.45 Å resolution, the highest resolution published for PNPs so far. The crystals contain the full PNP homotrimer in the asymmetric unit. DFPP-DG molecules are bound in superimposable manner and with full occupancies to all three PNP subunits. Thus the postulated third-of-the-sites binding of immucillins should be rather attribute to the second feature of the transition state, ribooxocarbenium ion character of the ligand or to the coexistence of both features characteristic for the transition state. The DFPP-DG/PNP complex structure confirms the earlier observations, that the loop from Pro57 to Gly66 covering the phosphate-binding site cannot be stabilized by phosphonate analogues. The loop from Glu250 to Gln266 covering the base-binding site is organized by the interactions of Asn243 with the Hoogsteen edge of the purine base of analogues bearing one feature of the postulated transition state (protonated N7 position).

Introduction

Purine nucleoside phosphorylases (PNP, E.C. 2.4.2.1) catalyze the conversion of β-purine nucleoside and orthophosphate to purine base and α-D-pentose-1-phosphate. Mammalian purine nucleoside phosphorylases belong to the so-called low molecular mass PNPs that are characterized by a homotrimeric architecture and a strong preference for guanosine and inosine over adenosine. High-molecular mass PNPs are trimers of dimers and accept all three nucleosides as substrates [1]. Ribooxocarbenium ion character of the pentose is one of the transition state features of low- and high-molecular mass PNPs. However, the ionic state of the base is still a point of some controversy, with protonation of the purine ring position N7 being the most widely accepted mechanism for hexameric PNPs, and one of the postulated mechanisms for trimeric PNPs [1–4].

Abbreviations: PNP, purine nucleoside phosphorylase; DFPP-DG, 9-(5′,5′-difluoro-5′-phosphonopentyl)-9-deazaguanine; DFPP-G, 9-(5′,5′-difluoro-5′-phosphonopentyl)-guanine; Hx, hypoxanthine; ImmH, immucillin H; Ino, inosine; Hepes, *N*-[2-hydroxyethyl]piperazine-N'-[2-ethanesulfonic acid]; U, enzyme activity unit; K_d, dissociation constant; A.U., arbitrary units

* Corresponding author. Fax: +48 22 554 0771.
E-mail address: abzowska@biogeo.uw.edu.pl (A. Bzowska).

0006-291X/$ - see front matter © 2009 Elsevier Inc. All rights reserved.
doi:10.1016/j.bbrc.2009.11.124

Human PNP has became an important drug target after it was shown that lack of its activity leads to selective immunodeficiency resulting from incorrect T-cell proliferation [1]. For *in vivo* efficiency, PNP inhibitors require a dissociation constant of 10 nM or lower [5]. Due to the charged nature of one part of the PNP substrate (orthophosphate), many PNP inhibitors, multisubstrate analogue inhibitors, carry a negative charge. They are therefore problematic for an *in vivo* use, because they cannot effectively penetrate cell membranes. By contrast transition state analogue inhibitors, immucillins, carry a positive charge, but thanks to the p*K* of protonation close to neutral pH (p*K* = 6.9), they can pass through the membranes with high efficiency [4]. Most likely they transverse the membrane in the neutral form and get protonated inside the cell. Immucillins bind to PNP with pronounced negative cooperativity. This effect has been called "third-of-the-sites binding", because two substrate binding sites of the trimeric enzyme remain unoccupied over a wide range of inhibitor concentrations. Quantitatively, the dissociation constant for the first site is in the pM range, while dissociation constants for the two remaining sites are orders of magnitude higher [6,7]. Thanks to the excellent properties of these inhibitors (membrane permeability, tight binding), one of them, immucillin H, is now in clinical trials [8,9] and has recently been reported to be quite efficient in treatment of T-cell leukaemia [e.g. 10].

As a result of our continuous search for efficient PNP inhibitors for *in vivo* applications and studies of the enzyme catalytic mechanism, we synthesized molecules that combine features of the transition state (protonated N7 position of the base) and multisubstrate analogues. Molecules built of the 9-deazaguanine alkyl-linked to the difluoromethylenephosphonate proved to be potent inhibitors of mammalian PNPs [11,12]. The promising biochemical results prompted us to determine the X-ray structure of the recombinant calf PNP complexed with one of such compounds 9-(5′,5′-difluoro-5′-phosphonopentyl)-9-deazaguanine (DFPP-DG). Crystals diffracted to 1.45 Å, which is the best resolution reported for any trimeric PNP. Up to now, all structures of the enzyme in complex with immucillins [13], as well as the only structure [14] of its complex with 9-deaza multisubstrate analogue inhibitor (PDB code 2ai2), contained one monomer in the asymmetric unit. Therefore, possible differences between subunits resulting from the third-of-the-sites binding effect, could not be observed. By contrast, the full PNP trimer was present in the asymmetric unit of the structure of DFPP-DG/PNP complex presented here, which thus proved suitable to study this phenomenon. Even if the effect did not have influence on the shape of the entire PNP molecule, low occupancy of the ligand should be detectable.

Materials and methods

Chemicals. Recombinant calf PNP was obtained as described previously [15]. The enzyme had the specific activity of about 34 U/mg, i.e. exactly the same as the 100% active non-recombinant calf spleen PNP [16], which suggests that all its molecules were active. This was essential to assure that the stoichiometry of binding reported in this work was correct. DFPP-DG was synthesized as described before [11]. Inosine (Ino), Hepes (ultra pure), polyethylene glycol, β-octylglucopyranoside and xanthine oxidase from buttermilk (a suspension in 2.3 M ammonium sulfate with specific activity of 1 U/mg at 25 °C) were from Sigma, Tris and magnesium chloride was from Roth. All solutions were prepared with MilliQ water.

Instrumentation. Spectrophotometric measurements were carried out in 10-mm path length quartz cuvettes (Hellma, Germany), on the Uvikon 930 (Kontron, Austria) and Cary 100 (Varian, USA) spectrophotometers with the thermostatically controlled cell compartments. The Beckman model Φ300 pH-meter equipped with a combined semi-microelectrode and temperature sensor was used for pH determination. Fluorescence data were recorded on the Perkin-Elmer LS-55 spectrofluorimeter (Norwalk, CT, USA) using 4 × 10 mm cuvettes with continuous stirring of solution.

PNP activity. The specific enzyme activity was measured spectrophotometrically with Ino as the substrate using the standard coupled xanthine oxidase procedure with $\lambda_{obs} = 300$ nm and $\Delta\varepsilon = 9600\ M^{-1}\ cm^{-1}$ [17]. One unit of phosphorylase activity is defined as the amount of enzyme that causes phosphorolysis of one μmol of Ino to Hx and ribose-1-phosphate per minute under standard conditions (25 °C, 0.5 mM Ino, 50 mM sodium phosphate buffer pH 7.0).

Enzyme and ligand concentrations. PNP and DFPP-DG concentrations were determined spectrophotometrically with the following extinction coefficients: $\varepsilon^{1\%}_{PNP}(280\ nm) = 9.6\ cm^{-1}$ [17], $\varepsilon_{DFPP\text{-}DG}(280\ nm) = 10\ 100\ M^{-1}cm^{-1}$ at pH 7.0 [11]. Molar concentration of PNP was always given for a monomer for direct comparison with molar concentration of the ligand. In all calculations, the theoretical molecular mass of a monomer of the calf enzyme based on its amino acid sequence (284 residues) was used, $M_r = 31{,}654$ Da.

Fluorescence titrations. Fluorescence data were collected at 25 °C, with excitation and observation wavelengths, $\lambda_{exc} = 290$ nm and $\lambda_{obs} = 350$ nm, respectively. The path length for excitation was 4 mm and that for emission 10 mm. Dilution did not exceed 15%, and fluorescence intensity was corrected for the dilution factor. Inner filter effect was negligible.

The binding was well described by a single dissociation constant. The following equation was used to obtain dissociation constant and the stoichiometry of binding [18]:

$$F([L]) = F_0 - (f_E - f_{EL} + f_L)\left(\frac{[L]}{2} + \frac{[E_{act}]}{2} + \frac{K_d}{2} - \frac{\sqrt{([L] - [E_{act}] + K_d)^2 + 4[E_{act}]K_d}}{2}\right) + [L]f_L \quad (1)$$

Parameters f_E, f_L and f_{EL} are fluorescence coefficients of free PNP, free DFPP-DG and PNP complexed with DFPP-DG, respectively, [L] is the total concentration of DFPP-DG, F([L]) is the fluorescence intensity observed for the ligand concentration [L], $[E_{act}]$ is the total concentration of the enzyme binding sites, and F_0 is the initial fluorescence intensity of the protein and buffer mixture before titration. Non-linear regression analysis was used, giving values for five fitted parameters: K_d, $[E_{act}]$, F_0, f_L and $(f_E - f_{EL} + f_L)$ (Fig. 1).

Crystallization. Recombinant calf PNP (10 mg/ml, about 310 μM subunit concentration) was complexed with DFPP-DG (660 μM). Hanging crystallization drops were set up at 20 °C temperature by mixing 3 μl of the PNP inhibitor complex in 1:2 ratio with 3 μl of the reservoir buffer (27% PEG 400, 0.02% sodium azide, 0.1 M Hepes pH 7.9, 0.1 M magnesium chloride) and allowed to equilibrate against reservoir buffer. Similar crystallization conditions for calf PNP have been described previously [19]. Typically, small (about 0.2 mm) dome-shaped crystals assigned to the cubic space group P 2_1 3 could be grown. In the case of the DFPP-DG/PNP complex, in addition to the known crystal form, large crystals of space group C 1 2 1 appeared in the drop. Particularly fine crystals of the new form were observed when 1% β-octylglucopyranoside was present in the buffer.

Crystal structure determination. The C 1 2 1 crystal form diffracted up to 1.45 Å on beamline BW6 at DESY (Deutsches Elektronen-Synchrotron, Hamburg, Germany). The diffraction data were integrated with MOSFLM [20] and scaled with SCALA [21]. Crystals contained one trimer of calf PNP in the asymmetric unit, and therefore test reflections for the R-free calculations were selected in thin resolution shells using DATAMAN [22]. The structure was solved by molecular replacement with the program MOLREP [23] using

Table 1
Data collection and refinement statistics for the crystal structure of calf PNP in complex with DFPP-DG. The atomic coordinates of the final model together with the corresponding structure factors were deposited in Protein Data Bank with the accession code 3fuc.

Space group	C 1 2 1
Unit cell dimensions	a = 135.79 Å b = 78.25 Å c = 94.90 Å β = 97.19°
No. of monomers/asymmetric unit	3
No. of unique reflections (all/test)	173,360/8787 (R-free set in thin resolution shells)
Resolution range [Å]	10.00–1.45
Completeness (last shell) [%]	99.4 (99.9)
I/σ (last shell)	11.7 (3.0)
R_{sym} (last shell) [%]	8.2 (23.6)
B-factor from Wilson plot [Å^2]	16.0
R-factor [%]	18.4
R-free [%]	20.7
rmsd bond lengths [Å]	0.011
rmsd angles [°]	1.37
Average B [Å^2]	18.3
Ramachandran core [%]	94.8
Ramachandran allowed [%]	4.8
Ramachandran add. allowed [%]	0.0
Ramachandran disallowed [%]	0.4

the trimeric form of the previously determined calf PNP structure (PDB code 1lv8, [24], ligand removed) as the search model. The structure was corrected manually in Coot [25] and refined using REFMAC [26] (Table 1). Non-crystallographic symmetry (NCS) restraints were not used during refinement. The DFPP-DG topology and parameter files were generated with the PRODRG web server [27]. Target parameters were used with standard weights as suggested by the PRODRG server.

Results and discussion

Binding of DFPP-DG to PNP

As a first step, we determined the dissociation constant and binding stoichiometry of the new ligand, 9-(5′,5′-difluoro-5′-phosphonopentyl)-9-deazaguanine (DFPP-DG, Fig. 1) with calf PNP in solution by fluorimetric titration. To maintain the strong fluorescence signal and determine the precise stoichiometry, we used the receptor concentration over 1000 times higher than the expected dissociation constant. The dissociation constants of extremely strong inhibitors such as DFPP-DG cannot be obtained by a single ligand titration approach, but replacement of a weaker ligand with the stronger one or a stopped-flow method needs to be applied. However, our goal was to precisely determine the binding stoichiometry, and not the dissociation constant. We have found that the model of non-interacting binding sites properly describes the binding of DFPP-DG to the enzyme (Fig. 1). The dissociation constant derived from fitting of this model to the data gives K_d = (190 ± 90) pM. The observed stoichiometry is one ligand molecule per PNP monomer. A third-of-the-sites effect is not observed, even though the dissociation constant for DFPP-DG is comparable to that of immucillins, which show K_d in the pM range [e.g. 6,7].

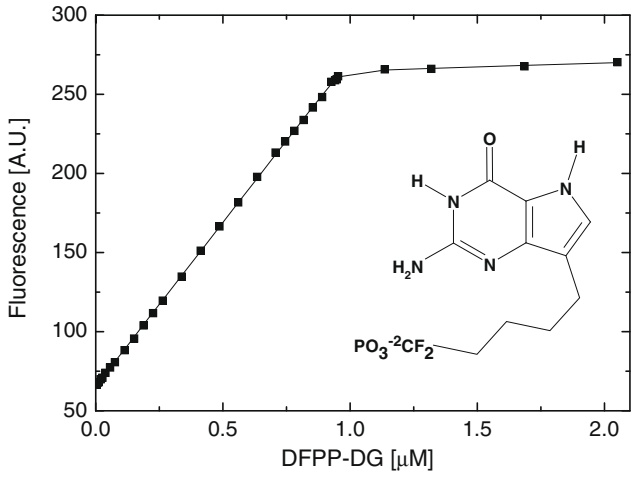

Fig. 1. Fluorimetric titrations of PNP with DFPP-DG in 20 mM Hepes buffer pH 7.0, 25 °C. The concentration of the enzyme subunits was (0.9 ± 0.1) μM. Titration data were fitted to Eq. (1) shown in Materials and Methods. The fitted parameters equaled: K_d = (190 ± 90) pM; [E_{act}] = (0.96 ± 0.1) μM; f_L = (4.89 ± 1.00) A.U., (f_E–f_{EL} + f_L) = (65.5 ± 0.3) A.U., F_0 = (65.5 ± 0.2) A.U. Insert: schematic diagram of DFPP-DG.

Overall structure of the PNP/DFPP-DG complex

The C 1 2 1 crystals contained one trimer of calf PNP in complex with DFPP-DG in the asymmetric unit. The overall structure of the enzyme is very similar to the one previously observed for PNP crystallized in space group $P2_12_12_1$ (with two full trimers in the asymmetric unit) in complex with different ligands, and in the presence or absence of phosphate (PDB codes 1lvu and 1lv8, [24]). Quantitatively the main chain residues in these structures (whole trimer, 852 residues) may be superimposed with pairwise rmsd of less than 1.15 Å.

The crystallographic data are in perfect agreement with the fluorimetric results and also do not support the third-of-the-sites binding. DFPP-DG molecules are bound to all three subunits. Superposition of the ligands bound to the three monomers demonstrates that the enzyme-inhibitor interactions are essentially identical (not shown). Even if the preference of one site over the others would not influence the overall shape of the PNP molecule and the differences between monomers get averaged out in the diffraction process, we should be able to detect the phenomenon by ligand occupancies lower than 1 (approximately 0.3), which is not the case. The group occupancy refinement carried out with the program CNS [28] confirms occupancies of around 1 for all three ligand molecules.

Base-binding site

Since the three ligand-binding sites do not display significant differences, it suffices to discuss one representative example only (monomer A, Fig. 2). The base-binding site is occupied by the 9-deazaguanine group of DFPP-DG inhibitor. In the parent compound (guanine), the N9 atom is sp2-hybridized and contributes a lone pair of electrons to the aromatic system of the base. The N to C substitution is expected to shift a double bond to preserve the aromatic state and planarity of the base. The high resolution of the presented crystal structure made it possible to confirm this experimentally. Irrespective of the refinement restraints (no restraint, sp2 or sp3 with standard weight), the base refined to a planar structure (data not shown). Due to the formally shifted double bond, 9-deazaguanine has an NH group in the position of the guanine N7 atom. The extra H atom is thought to mimic a feature of the transition state (albeit without the positive charge), and enables the favorable interaction between the Hoogsteen edge of 9-deazaguanine and Asn243. The interaction involves two hydrogen bonds with very favorable geometry, one from the NH group of 9-deazaguanine to the Oδ atom of the side chain of Asn243, and another one from the Nδ atom of this amino acid to the O6 atom of the inhibitor (Fig. 2). On the Watson–Crick edge, 9-deazaguanine forms the two hydrogen bonds with Glu201 that

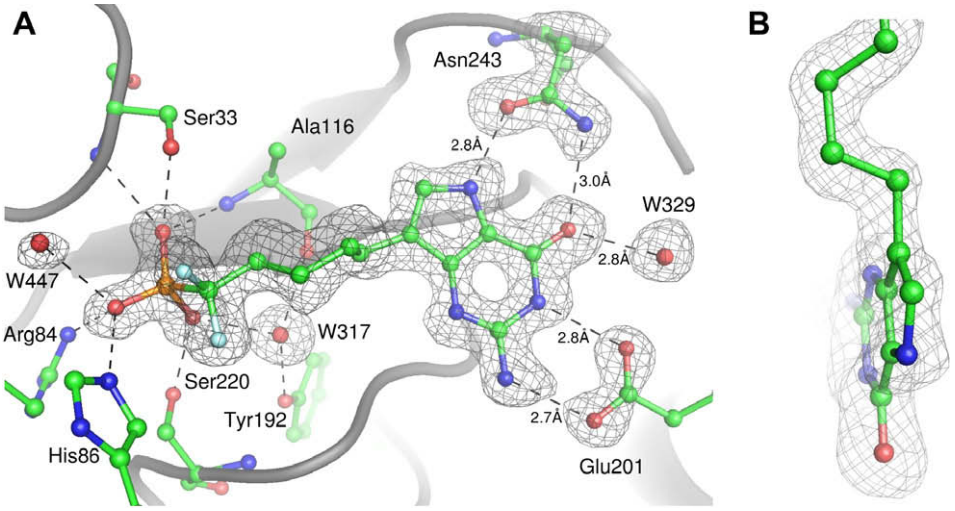

Fig. 2. (A) Diagram of the interactions between DFPP-DG and calf PNP. For clarity only selected residues are presented in a full atom representation. Composite omit $|2F_o-F_c|$ electron density map contoured at 2.0σ is shown for the inhibitor, base binding residues and most important water molecules (denoted as "W"). Hydrogen bonds are indicated by dashed lines. For the enzyme-base interactions the corresponding interatomic distances are stated. (B) Side view of the DFPP-DG molecule along with the composite omit map contoured at 2.0σ level. The planar geometry of C9 position can be clearly seen. The figures were prepared in PyMOL [34]. Simulated annealing refinement to minimize model bias was performed with CNS [28] with the starting temperature of 500 K.

are routinely seen in co-crystal structures of PNPs with guanine and acyclic nucleosides with guanine as an aglycone [1].

Phosphate and ribose-binding sites

The phosphate-binding site is occupied by the CF_2-phosphonate as expected. The phosphonate group interacts with the side chains of Ser33, Arg84, His86 and Ser220, as well as with the main chain nitrogen atoms of Ser33 and Ala116. These interactions are analogous to the previously observed contacts of calf spleen PNP in the structures with co-substrates ribose-1-phosphate and phosphate or its analogue sulfate. The only exception is His64, reported to be in the vicinity of the active site (e.g. 1a9s, 1a9t [29], 1b80 [13] and 1fxu [30]), and disordered in the present structure, and also in the other complexes with phosphonate group mimicking phosphate (e.g. 1v48, [31]). A very well-ordered water molecule (W317) bridges the phosphonate, the Tyr192 OH group and the Ala116 carbonyl oxygen atom, as in all other calf PNP structures. The alkyl linker connecting CF_2-phosphonate with 9-deazaguanine occupies the ribose-binding site. The linker is not engaged in specific interactions with the enzyme. Similar results were obtained for 9-aza analogue of DFPP-DG, DFPP-G (1v48 [31]).

57–66 loop conformation

The loop from Pro57 to Gly66 could not be reliably traced in our structure. In previous PNP structures, this loop has been observed in various states of order. It was disordered in the structure of the binary complex of PNP with Hx (PDB code 1vfn, [32] and in the complexes of PNP with multisubstrate analogue inhibitors, in which phosphonate mimicked phosphate (2ai1, 2ai2, 2ai3, [14]). In contrast, it was ordered in the structures with a phosphate or sulfate molecule bound in the PNP phosphate-binding site: PNP/PO_4 complex (4pnp), PNP/Hx/SO_4 complex (1a9r), PNP/Hx/SO_4 (1a9s), PNP/9-deaza-Ino/SO_4 (1a9p), PNP/ribose-1-phosphate/Hx (1a9t [29]), PNP/N(7)-acycloguanosine/PO_4 (1fxu [30]), and PNP/ImmH/PO_4 (1b8o, [13])). The loop could also be built with high B-factors in one structure of unliganded PNP (1pbn [29]) and in two other structures (1lvu, 1lv8 [24]) where it was trapped by crystal contacts. Disregarding these special cases, it appears that binding of phosphate or sulfate anchors His64 and this residue then "locks in" the entire loop. The present structure together with the previous complexes of PNP with multisubstrate analogues, suggest that phosphonate cannot substitute for a sulfate or phosphate to stabilize this loop.

250–266 loop conformation

The loop comprising residues Glu250 to Gln266 covers the base-binding site. In the structure described here the N7 position of the ligand is protonated and the 250–266 loop appears well-ordered (Fig. 3). The loop is anchored by a chain of well-ordered

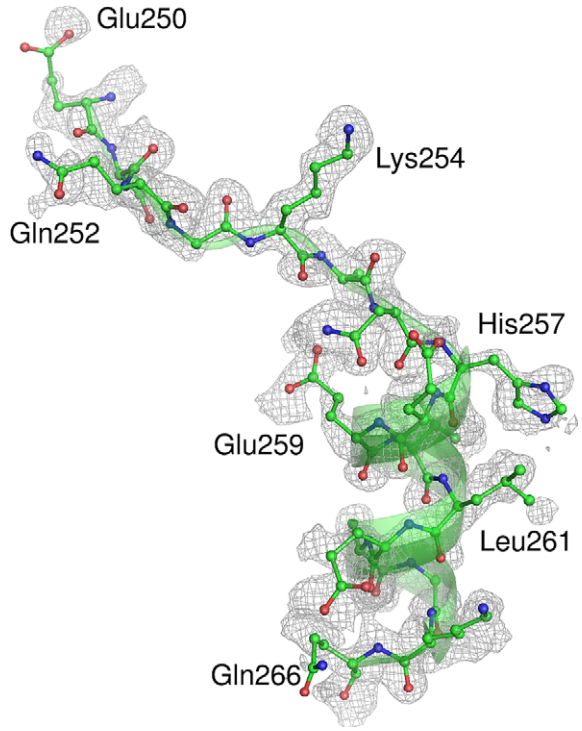

Fig. 3. Composite omit $|2F_o-F_c|$ electron density map (contoured at 2.0σ) for the region between Glu250 and Gln266. The composite omit map were calculated with CNS [28]. Prepared in PyMOL [34].

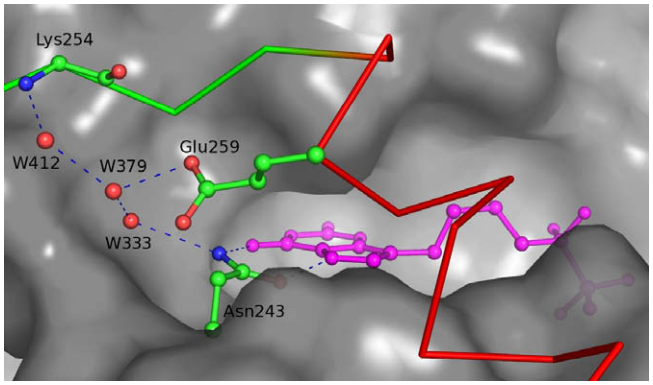

Fig. 4. Chain of well-ordered water molecules (W333, W379, W412) anchoring Glu259 and Lys254 to Asn243. Prepared in PyMOL [34].

water molecules with low temperature factors, supported by the interactions of one of them with Asn243 (Fig.4). It might suggest that some reduction in the degree of freedom of enzyme and/or ligand occurs in this case. This would be in agreement with our earlier calorimetric results suggesting that the entropic contribution to PNP binding was less favorable for DFPP-DG than for DFPP-G [33]. The conformation and flexibility of the 250–266 loop correlates with the presence of a hydrogen bond donor at the N7 position of the base. In all known structures with the N7 atom protonated, the loop is well organized, and it is usually disordered in the ones with this position not protonated. The ligands of structures 2ai1 [14] and 1a9s [29] should be unprotonated in solution at neutral pH. However, the conformations of the Asn243 residues in the co-crystal structures identify the N7 atoms as protonated, and the loops are ordered in agreement with the rule.

The structure presented here is consistent with the suggestion derived from previous studies that the NH group at the N7 position orients the side chain of Asn243. This residue forms two hydrogen bonds with the Hoogsteen edge of the base part of the ligand, which in turn "locks in" the 250–266 loop that covers the base-binding site. The effect may be achieved either as a result of 9-deaza modification in analogues of the postulated transition state, or as a result of the protonation of the natural substrate, inosine, in the course of catalysis. In the first case the loop is more rigid, reflecting the stable incorporation of the transition state feature into the ligand structure. By contrast, in the second case the loop is a bit more flexible, reflecting the transient nature of the transition state of the natural substrate during the enzymatic reaction. This conclusion would be in agreement with the N7 protonation mechanism of catalysis suggested by Fedorov et al. [13] as one possible reaction path.

Acknowledgments

This work was supported by the Polish Ministry of Science and Higher Education (Grants N301 003 31/0042 and BW-1724/BF). Dr. Hans Bartunik is gratefully acknowledged for generous access to the beamline BW6 at DESY, Hamburg, and Mrs. Lucyna Magnowska for the excellent technical assistance.

References

[1] A. Bzowska, E. Kulikowska, D. Shugar, Purine nucleoside phosphorylases: properties, functions, and clinical aspects, Pharmacol. Ther. 88 (2000) 349–425.
[2] J. Tebbe, A. Bzowska, B. Wielgus-Kutrowska, Z. Kazimierczuk, W. Schröder, D. Shugar, W. Saenger, G. Koellner, Crystal structures of purine nucleoside phosphorylase (PNP) from *Cellulomonas* sp., and its implications for the molecular mechanism of trimeric PNPs, J. Mol. Biol. 294 (1999) 1239–1255.
[3] G. Koellner, A. Bzowska, B. Wielgus-Kutrowska, M. Luić, T. Steiner, W. Saenger, J. Stępiński, Open and closed conformation of the *E. coli* purine nucleoside phosphorylase active center and implications for the catalytic mechanism, J. Mol. Biol. 315 (2002) 351–371.
[4] A.A. Sauve, S.M. Cahill, S.G. Zech, L.A. Basso, A. Lewandowicz, D.S. Santos, C. Grubmeyer, G.B. Evans, R.H. Furneaux, P.C. Tyler, A. McDermott, M.E. Girvin, V.L. Schramm, Ionic states of substrates and transition state analogues at the catalytic sites of *N*-ribosyltransferases, Biochemistry 42 (2003) 5694–5705.
[5] J.D. Stoeckler, Purine nucleoside phosphorylase: a target for chemotherapy, in: R.J. Glazer (Ed.), Developments in Cancer Chemotherapy, CRC Press Inc., Boca Raton, FL, 1984, pp. 35–60.
[6] R.W. Miles, P.C. Tyler, R.H. Furneaux, C.K. Bagdassarian, V.L. Schramm, One third-the-sites transition-state inhibitors for purine nucleoside phosphorylase, Biochemistry 37 (1998) 8615–8621.
[7] A.A. Edwards, J.M. Mason, K. Clinch, P.C. Tyler, G.B. Evans, V.L. Schramm, Altered enthalpy–entropy compensation in picomolar transition state analogues of human purine nucleoside phosphorylase, Biochemistry 48 (2009) 5226–5238.
[8] F. Ravandi, V. Gandhi, Novel purine nucleoside analogues for T-cell-lineage acute lymphoblastic leukaemia and lymphoma, Expert Opin. Investig. Drugs 15 (2006) 1601–1613.
[9] K. Balakrishnan, R. Nimmanapalli, F. Ravandi, M.J. Keating, V. Gandhi, Forodesine, an inhibitor of purine nucleoside phosphorylase, induces apoptosis in chronic lymphocytic leukemia cells, Blood 108 (2006) 2392–2398.
[10] M. Huang, Y. Wang, J. Gu, J. Yang, K. Noel, B.S. Mitchell, V.L. Schramm, L.M. Graves, Determinants of sensitivity of human T-cell leukemia CCRF-CEM cells to immucillin-H, Leuk. Res. 32 (2008) 1268–1278.
[11] S. Hikishima, M. Hashimoto, L. Magnowska, A. Bzowska, T. Yokomatsu, Synthesis and biological evaluation of 9-deazaguanine derivatives connected by a linker to difluoromethylene phosphonic acid as multisubstrate analogue inhibitors of PNP, Bioorg. Med. Chem. Lett. 17 (2007) 4173–4177.
[12] T. Yatsu, M. Hashimoto, S. Hikishima, L. Magnowska, A. Bzowska, T. Yokomatsu, 9-Deazaguanine derivatives, synthesis and inhibitory properties as multi-substrate analogue inhibitors of mammalian PNPs, Nucleic Acids Symp. Ser. (Oxf) 52 (2008) 661–662.
[13] A. Fedorov, W. Shi, G. Kicska, E. Fedorov, P.C. Tyler, R.H. Furneaux, J.C. Hanson, G.J. Gainsford, J.Z. Larese, V.L. Schramm, S.C. Almo, Transition state structure of purine nucleoside phosphorylase and principles of atomic motion in enzymatic catalysis, Biochemistry 40 (2001) 853–860.
[14] A.V. Toms, W. Wang, Y. Li, B. Ganem, S.E. Ealick, Novel multisubstrate inhibitors of mammalian purine nucleoside phosphorylase, Acta Crystallogr. D 61 (2005) 1449–1458.
[15] K. Breer, A. Girstun, B. Wielgus-Kutrowska, K. Staroń, A. Bzowska, Overexpression, purification and characterization of functional calf purine nucleoside phosphorylase (PNP), Protein Expr. Purif. 61 (2008) 122–130.
[16] A. Bzowska, Calf spleen purine nucleoside phosphorylase: complex kinetic mechanism, hydrolysis of 7-methylguanosine, and oligomeric state in solution, Biochim. Biophys. Acta 1596 (2002) 293–317.
[17] J.D. Stoeckler, R.P. Agarwal, K.C. Agarwal, R.E. Parks Jr., Purine nucleoside phosphorylase from human erythrocytes, Methods Enzymol. 51 (1978) 530–538.
[18] M.R. Eftink, Fluorescence methods for studying equilibrium macromolecule-ligand interactions, Methods Enzymol. 278 (1997) 221–257.
[19] A. Bzowska, M. Luić, W. Schröder, D. Shugar, W. Saenger, G. Koellner, Calf spleen purine nucleoside phosphorylase: purification, sequence and crystal structure of its complex with an N(7)-acycloguanosine inhibitor, FEBS Lett. 367 (1995) 214–218.
[20] A.W.G. Leslie, Recent changes to the MOSFLM package for processing film and image plate data, Joint CCP4 + ESFEAMCB, Newslett. Protein Crystallogr. 26 (1992).
[21] Collaborative Computational Project Number 4. The CCP4 Suite: Programs for Protein Crystallography, Acta Cryst. D50 (1992) 760–763.
[22] G.J. Kleywegt, T.A. Jones, XdlMAPMAN and xdlDATAMAN - programs for reformatting, analysis and manipulation of biomacromolecular electron-density maps and reflection data sets, Acta Cryst. D52 (1996) 826–828.
[23] A. Vagin, A. Teplyakov, A.MOLREP: an automated program for molecular replacement, J. Appl. Cryst. 30 (1997) 1022–1025.
[24] A. Bzowska, G. Koellner, B. Wielgus-Kutrowska, A. Stroh, G. Raszewski, A. Holý, T. Steiner, J. Frank, Crystal structure of calf spleen purine nucleoside phosphorylase with two full trimers in the asymmetric unit: important implications for the mechanism of catalysis, J. Mol. Biol. 342 (2004) 1015–1032.
[25] P. Emsley, K. Cowtan, Coot: Model-Building Tools for Molecular Graphics, Acta Cryst. D60 (2004) 2126–2132.
[26] G.N. Murshudov, A.A. Vagin, E.J. Dodson, Refinement of macromolecular structures by the maximum-likelihood method, Acta Cryst. D53 (1997) 240–255.
[27] A.W. Schuettelkopf, D.M.F. Van Aalten, PRODRG - a tool for high-throughput crystallography of protein-ligand complexes, Acta Cryst. D60 (2004) 1355–1363.
[28] A.T. Brunger, P.D. Adams, G.M. Clore, W.L. DeLano, P. Gros, R.W. Grosse-Kunstleve, J.-S. Jiang, J. Kuszewski, N. Nilges, N.S. Pannu, R.J. Read, L.M. Rice, T. Simonson, G.L. Warren, Crystallography and NMR system (CNS): a new software system for macromolecular structure determination, Acta Cryst. D54 (1998) 905–921.

[29] C. Mao, W.J. Cook, M. Zhou, A.A. Federov, S.C. Almo, S.E. Ealick, Calf spleen purine nucleoside phosphorylase complexed with substrates and substrate analogues, Biochemistry 37 (1998) 7135–7146.
[30] M. Luić, G. Koellner, D. Shugar, W. Saenger, A. Bzowska, Calf spleen purine nucleoside phosphorylase: structure of its ternary complex with an *N*(7)-acycloguanosine inhibitor and a phosphate anion, Acta Cryst. D57 (2001) 30–36.
[31] M. Luić, G. Koellner, T. Yokomatsu, S. Shibuya, A. Bzowska, Calf spleen purine-nucleoside phosphorylase: crystal structure of the binary complex with a potent multisubstrate analogue inhibitor, Acta. Cryst. D 60 (2004) 1417–1424.
[32] G. Koellner, M. Luić, D. Shugar, W. Saenger, A. Bzowska, Crystal structure of the calf spleen purine nucleoside phosphorylase in a complex with hypoxanthine at 2.15 Å resolution, J. Mol. Biol. 265 (1997) 202–216.
[33] K. Breer, B. Wielgus-Kutrowska, M. Hashimoto, S. Hikishima, T. Yokomatsu, R. Szczepanowski, M. Bochtler, A. Girstun, K. Staroń, A. Bzowska, Thermodynamic studies of interactions of calf spleen PNP with acyclic phosphonate inhibitors, Nucleic Acids Symp. Ser. 52 (2008) 663–664.
[34] W.L. DeLano, The PyMOL Molecular Graphics System, 2002, Available from <http://www.pymol.org>.